Asteroid Exploration using a Small Space-Robot subject to Hybrid Actuators

Aishashwini[1] * **Vikram Kumar Saini**[2] * **Ankit M Patel**[3] *
Shashi Ranjan Kumar[4] ** **Dipak Kumar Giri**[5] *

* *Department of Aerospace Engineering, Indian Institute of Technology Kanpur, Uttar Pradesh - 208016, INDIA.*
** *Department of Aerospace Engineering, Indian Institute of Technology Bombay, Maharashtra - 400076, INDIA.*

Abstract: This paper proposes an idea for configuration of actuators for a small space robot for asteroid exploration using coupled dynamics of attitude and position. Space-robot configuration includes variable-speed control moment gyroscope (VSCMG), reaction wheel (RW) and a body fixed thruster. Since a single body fixed thruster cannot have the full position control, so the problem is under actuated, and this makes it a coupled problem of attitude and position control. A stable PID control law is developed for position control and sliding mode using Modified Rodrigues Parameter (MRP) is used for developing the control law for attitude control. The closed loop stability of the system is proven using Lyapunov stability criteria for attitude control. The asteroid gravity is modelled by taking an arbitrary shaped asteroid. In this paper maneuvering and hovering is performed using the proposed design. Finally the simulations and results are demonstrated for showing the effectiveness of the proposed actuator configuration for maneuvering and hovering a space-robot.

Keywords: Variable-speed control moment gyroscope (VSCMG), sliding mode, gravity modelling, Modified Rodrigues Parameter (MRP).

1. INTRODUCTION

In recent years, near earth asteroids and comets have attracted a lot of attention because it is thought that they may still contain some remnants of the time when our solar system first formed. Studying the basics of asteroids may provide us insight into the early stages of planet formation and, more importantly, it can assist us in gathering information about the threat that asteroids pose to Earth. Exploration of an arbitrary shaped asteroid using a large spacecraft, will be expensive and challenging. Instead, a small spacecraft such as space robot or CubeSat can explore variety of areas of both small and large asteroid effectively. Small spacecrafts are already attracting attention because they allow us to explore space to a larger degree. A wide variety of high-quality sensors and actuators are now readily available, which is causing development in the field of small spacecraft to accelerate. However, efforts to create a superior actuator technology are currently ongoing.

There are various types of actuators available for spacecraft control, such as magnetic rods, torque coils, reaction wheel, chemical and electric thrusters, and Control Moment Gyroscopes (CMGs). Due to their light weight and high torque amplification, a CMG acts as very promising actuator for small satellite missions (Tayebi et al. [2017]). There are several types of CMGs, among which VSCMGs are the most powerful actuator as they can generate significant torque with less energy consumption and also can vary wheel's speed continuously (Lungu and Lungu [2019]). VSCMG is combination of RW and control moment gyroscope (CMG). Although CMG's are more power-efficient than RWs, their control laws have singularity issues, while RWs are not able to work at high torque levels and frequently desaturate (Cornick [1979], Margulies [1978], Ismail and Varatharajoo [2010]). RWs are expensive but efficient actuator that has been widely employed to control the attitude of both large and small satellites (Brieß et al. [2005]). Nearly all satellite missions using RW for attitude control shows that a high attitude control performance can be attained with RW. In case of complete attitude control, the minimal actuator that can be used for position control is a single fixed thruster. Both chemical (discontinuous) and electric (continuous) thruster can be used as actuators, but for for small spacecrafts such as CubeSat, electric thrusters are preferred, as they reduce the total mass of spacecraft in large amount. In (Biggs and Livornese [2020]) authors are using more under-actuated system, as they are using only a single VSCMG and an electric thruster for control, because that work is concerned with a rendezvous problem which does not necessitate the rotational motion control about longitudinal axis. But for the problem of asteroid exploration, rotation about the longitudinal axis of the spacecraft is required to controlled for orienting camera

* [1] Under-Graduate Student
** [2] Ph.D Student, Flight Mechanics and Control, vksaini.1997@gmail.com
* ** [4] Assistant Professor, srk@aero.iitb.ac.in
* ** [5] Assistant Professor, dkgiri@iitk.ac.in

in some specific direction. Therefore, a new actuator configuration presented with an additional RW.

In this paper an idea is proposed on a high maneuvering actuator configuration equipped with VSCMG, reaction wheel and a fixed electric thruster. This configuration provides high maneuvering with full attitude control and under-actuated position control using minimal number of actuators. Since we only have one electric thruster available for position control, two loops are used to design the control laws for this problem. The orbital maneuvering begins with the implementation of a feedback control in the outer loop, where the necessary thrust can be generated to attain the desired position. Additionally, the inner loop uses VSCMG and RW to track the required acceleration. Near the asteroid, its gravity field cannot be ignored, which is non-spherical, so a gravity model for non-spherical body is used.

Rest of the paper is structured as follow. Section 2 presents problem which we are going to solve in rest of the paper and how we are planning to approach this problem. Section 3 shows the dynamics and kinematics to of the rigid body system, use of Modified Rodrigues Parameter. Control design for the space robot using sliding mode and PID control is presented in section 4. Section 5 and 6 demonstrate the stability analysis of the system and simulation results. Finally in section 7 we conclude the paper while suggesting further improvement that could be considered in future work. In the next section problem is discussed, on which we are working.

2. PROBLEM FORMULATION

This study seeks to explore an asteroid utilizing a compact spacecraft-robot with a single body fixed thruster, a single VSCMG, and a single RW for attitude and position control. The space robot is controlled in pitch and yaw by VSCMG, and in yaw by RW. Robot is supposed to begin navigating from someplace in space in the vicinity of asteroid and is desired to arrive at the targeted location close to the asteroid as depicted in Figure. (1). The main challenge in this problem is to control the position of the space-robot in the inertial-frame which located at the centre of the asteroid. Accurate position and attitude control is required in real application because of our interest in capturing the images of certain areas on asteroid surface and it is also desired that spacecraft orient its camera towards certain areas of interest on the asteroid surface.

3. KINEMATICS AND DYNAMICS OF SPACE ROBOT

For deriving the equations of the system, body is assumed to be rigid body. Body frame with its origin at the centre of mass of the robot is defined as $B = \{\widehat{b}_1, \widehat{b}_2, \widehat{b}_3\}$, first VSCMG frame is defined as $G = \{\widehat{s}_1, \widehat{t}_1, \widehat{g}_1\}$, where G frame is attached to gimbal, and RW frame is defined as $R = \{\widehat{s}_2, \widehat{t}_2, \widehat{g}_2\}$, as shown in Fig. (2). Asteroid frame or inertial frame is defined as $I = \{\widehat{i}, \widehat{j}, \widehat{k}\}$ with its origin located at the centre of the asteroid, as shown in Fig. (1). Now, in the subsection below kinematics and dynamics of the body are derived.

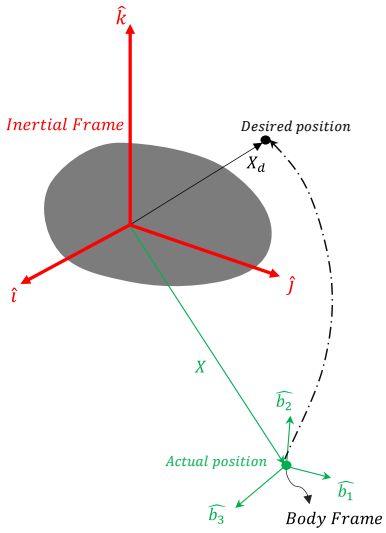

Fig. 1. Frames of Reference

3.1 Kinematics of Space Robot

Motion of the space robot is described in two frames, body frame and asteroid frame (i.e., inertial frame). Inertial frame and body frame of the system are described in Fig. (1). For the transformation between these two frames, modified Rodrigues parameter (MRP) is used as attitude parameter. The following equation gives the relation between robot's velocity and position in inertial coordinates.

$$\dot{X} = V \tag{1}$$

Where $X = [x, y, z]^T$ is the position and $V = [v_1, v_2, v_3]^T$ is the velocity vector of space-robot in inertial frame. Kinematics of the MRP is given by the following equation

$$\dot{\sigma} = G(\sigma)\omega \tag{2}$$

Here, $\sigma = [\sigma_1, \sigma_2, \sigma_3]^T$ is the MRP that describes the attitude of the body frame of the space robot, $\omega = [\omega_1, \omega_2, \omega_3]^T$ is the angular velocity of the body frame with respect to inertial frame expressed in the body frame co-ordinates. $G(\sigma)$ is given as follows

$$G(\sigma) = \frac{1}{2}[I + \sigma^{\times} + \sigma\sigma^T - 0.5(1 - \sigma^T\sigma)I]$$

Here, $\sigma^{\times}$ is skew-symmetric matrix of σ and I is an identity matrix of appropriate dimension.

3.2 Dynamics of Space-Robot

Position dynamics of the space robot is derived by applying Newton's second law. Position dynamics of space robot in the inertial frame can be written as

$$\ddot{X} = a + g_a(X) \tag{3}$$

Here $a = [a_1, a_2, a_3]^T$ is acceleration due to thrust vector in inertial frame, and $g_a(X)$ is gravity of asteroid that is pulling the space-robot radially towards the centre of the asteroid, as function of position vector in asteroid frame. $g_a(X)$ can be achieved by partially differentiating non-linear gravity potential equation taken from (Hu and Scheeres [2008]), defined below

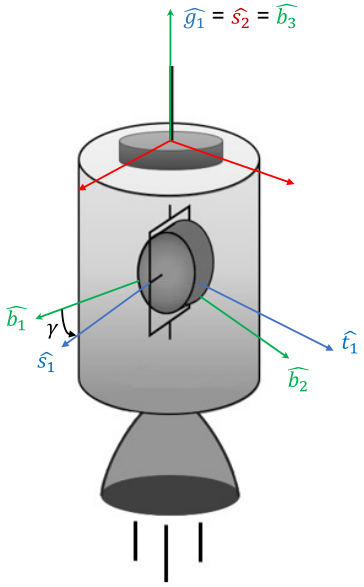

Fig. 2. Space robot model

$$U_g = \frac{1}{2}\omega_T^2(x^2+y^2) + \frac{\mu}{r} - \frac{\mu C_{20}(x^2+y^2-2z^2)}{2r^5} + ... \\ - \frac{3C_{22}(x^2-y^2)}{r^5} \quad (4)$$

Here, r is distance of robot from center of mass of asteroid is gravitational parameter, ω_T is rotation rate of asteroid about its $\widehat{k}$ axis (In this paper, it is assumed that asteroid is not rotating, therefore, $\omega_T = 0$) and C_{20} and C_{22} are gravity coefficients which can be expressed in terms of principal moments of inertia of the asteroid (normalized by the asteroid mass) I_{xx}, I_{yy} and I_{zz}.

$$C_{20} = -\frac{1}{2}(2I_{zz} - I_{xx} - I_{yy})$$

$$C_{22} = \frac{1}{4}(I_{yy} - I_{xx})$$

Thrust can be applied only in $\hat{b}_3$ direction in the body frame. Acceleration a that is computed in the inertial frame can be transformed from inertial frame to body frame using the the following equation

$$\begin{bmatrix} a_1 \\ a_2 \\ a_3 \end{bmatrix} = R_b^i \begin{bmatrix} 0 \\ 0 \\ T/m \end{bmatrix} \quad (5)$$

Here, T is thrust, m is the mass of space-robot, and R_b^i is the transformation matrix that transforms a vector from body frame to inertial frame, obtained from Euler angle rotation 3-2-1 between current acceleration vector and desired acceleration vector. R_b^i is given by the following equation

$$R_b^i = \begin{bmatrix} C\theta C\psi & S\phi S\theta C\psi - C\phi S\psi & C\phi S\theta C\psi + S\phi S\psi \\ C\theta S\psi & S\phi S\theta S\psi + C\phi C\psi & C\phi S\theta S\psi - S\phi C\psi \\ -S\theta & S\phi C\theta & C\phi C\theta \end{bmatrix} \quad (6)$$

Attitude dynamics of the system is derived from the conservation of angular momentum, that is, the derivative of angular momentum is zero when no external torque is applied. So, $\frac{dh}{dt}$ will be zero with respect to inertial frame.

$$^N\frac{dh}{dt} = 0 \quad (7)$$

Total angular momentum of robot in body frame will be due to inertia of whole body, angular momentum of VSCMG in gimbal axis, angular momentum of VSCMG in spin axis, angular momentum of RW in it spin axis. Total angular momentum of body can be expressed as follow.

$$h = J\omega + I_{1g}\dot{\gamma}\widehat{g}_1 + I_{1s}\Omega_1\widehat{s}_1 + I_{2s}\Omega_2\widehat{s}_2 \quad (8)$$

Here, $\omega = [\omega_1, \omega_2, \omega_3]^T$ is the angular velocity of the space robot with respect to inertial frame represented in the body frame, J is inertia matrix of spacecraft and I_{1g}, I_{1s} and I_{2s} are inertia of VSCMG about its gimbal axis, gimbaled RW about its spin axis and independent RW about its spin axis respectively and $\dot{\gamma}$, Ω_1 and Ω_2 are angular velocities of gimbal, gimbaled RW and second RW respectively. Time derivative of the total angular momentum vector in the body frame with respect to inertial frame can be written in the body frame axes using the transport theorem as follows

$$^N\frac{dh}{dt} = {}^B\frac{dh}{dt} + \omega \times h \quad (9)$$

$^B\frac{dh}{dt}$ can be found by differentiating Eq. (8) with respect to time in body frame. J is assumed to be constant,therefore, its time derivative will be zero, i.e. $\dot{J} = 0$. It should be noted that inertia matrix changes when gimbal angle of VSCMG varies. But it can be ignored as the the inertia of the gimbal system is much smaller compared to the inertia of the space robot. Double derivative of γ is also neglected as its contribution is small ($\ddot{\gamma} \sim 0$) (Yoon and Tsiotras [2006]). After doing all the necessary substitutions and computations using Eq. (9), Eq. (7) and Eq. (8), we get the following equation for rotational dynamics of the space robot

$$J\dot{\omega} = -\omega^{\times} J\omega + U + D \quad (10)$$

The terms U and D are given as follows

$$U = \begin{bmatrix} I_{1s}\Omega_1 sin\gamma - I_{1g}\omega_2 & I_{1s}cos\gamma & 0 \\ -I_{1s}\Omega_1 cos\gamma + I_{1g}\omega_1 & I_{1s}sin\gamma & 0 \\ 0 & 0 & -I_{2s} \end{bmatrix} \begin{bmatrix} \dot{\gamma} \\ \dot{\Omega}_1 \\ \dot{\Omega}_2 \end{bmatrix}$$

$$D = \begin{bmatrix} 0 & -I_{2s}\Omega_2 & I_{1s}\Omega_1 sin\gamma \\ I_{2s}\Omega_2 & 0 & -I_{1s}\Omega_1 cos\gamma \\ -I_{1s}\Omega_1 sin\gamma & I_{1s}\Omega_1 cos\gamma & 0 \end{bmatrix} \begin{bmatrix} \omega_1 \\ \omega_2 \\ \omega_3 \end{bmatrix}$$

The term U is utilized to compute the control inputs $\dot{\gamma}$, $\dot{\Omega}_1$ and $\dot{\Omega}_2$. The following section describes the design procedure of the control algorithm used for space robot position and attitude control.

4. CONTROL DESIGN

This is an under-actuated control problem since we have thruster only in one direction, therefore, there will be only four control inputs $\dot{\gamma}$, $\dot{\Omega}_1$, $\dot{\Omega}_2$ and T for six degree of freedom. To overcome this problem, we design the control in two loops, outer slow loop and inner fast loop. Outer loop generates the attitude commands for the inner loop for position tracking and inner loop ensures commanded attitude tracking. Here, we make use of the time scale separation principle, that is, inner loop control works on

higher natural frequency which means it is a fast loop, so that desired command generated by outer loop will get executed in inner loop faster before the next command is received from the slow outer loop. Block diagram for the control design is shown in Fig (3).

4.1 Outer Loop Design

For outer loop PID control law is used. Tracking error in position is $X_e = X - X_d$, here X and X_d are actual and desired position with respect to inertial frameas shown in Figure. (1). After applying PID control on acceleration due to thrust, we will get

$$a = -k_1 X_e - k_2 \dot{X}_e - k_3 \int X_e \tag{11}$$

Here, k_1, k_2 and k_3 are proportional, derivative and integral gains respectively. After putting back Eq. (11) in Eq. (3), we get the closed loop position dynamics as follows

$$\ddot{X} = -k_1 X_e - k_2 \dot{X}_e - k_3 \int X_e + g_a(X) \tag{12}$$

Using Eq. (3) and Eq. (5) we get desired thrust, desired pitch, yaw and roll in terms of Euler angles (Prabhakaran et al. [2015]).

$$T = m\sqrt{(g_{a1} - \ddot{x})^2 + (g_{a2} - \ddot{y})^2 + (g_{a3} - \ddot{z})^2}$$
$$\phi_d = sin^{-1}(psin\psi_d - qcos\psi_d)$$
$$\theta_d = sin^{-1}(\frac{pcos\psi_d + qsin\psi_d}{cos\phi_d})$$
$$\psi_d = 0$$

Here,

$$p = \frac{m(g_{a1} - \ddot{x})}{T}$$
$$q = \frac{m(g_{a2} - \ddot{y})}{T}$$

Since, in the current problem we are not re-orienting the space robot in its longitudinal axis ($\widehat{b}_3$), hence, ψ_d is taken to be zero. These commands are further converted into MRP by generating a rotation matrix (Eq. (6)) using commanded Euler angles and then converting the rotation matrix R back to MRP for inner loop using the following relation

$$\sigma = \begin{bmatrix}\sigma_1 \\ \sigma_2 \\ \sigma_3\end{bmatrix} = \frac{1}{\zeta(\zeta+2)}\begin{bmatrix}R_{23} - R_{32} \\ R_{31} - R_{13} \\ R_{12} - R_{21}\end{bmatrix} \tag{13}$$

Where,

$$\zeta = \sqrt{trace(R) + 1}$$

4.2 Inner Loop Design

Sliding mode control is used for the inner loop design. Let σ_e be the error in MRP defined as following

$$\sigma_e = \sigma - \sigma_d \tag{14}$$

The following sliding surface is chosen

$$s = \lambda\sigma_e + \dot{\sigma}_e \tag{15}$$

Where, $\lambda > 0$ is a positive constant. The dynamics of sliding surface is given as follows

$$\dot{s} = \lambda\dot{\sigma}_e + \ddot{\sigma}_e \tag{16}$$

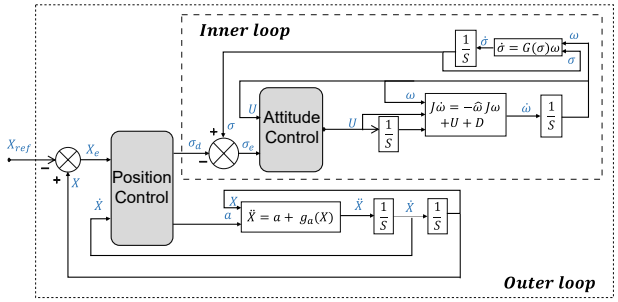

Fig. 3. Block diagram of control design

For converging the sliding surface dynamics to origin, the exponential reaching law is taken as follows

$$\dot{s} = -k_1 s - k_2 sign(s) \tag{17}$$

After differentiating Eq. (2) we get the following

$$\ddot{\sigma} = \dot{G}(\sigma)\omega + G(\sigma)\dot{\omega} \tag{18}$$

Here,

$$\dot{G}(\sigma) = \frac{1}{2}[\dot{\sigma}^{\times} + \dot{\sigma}\sigma^T + \sigma\dot{\sigma}^T - \dot{\sigma}^T\sigma I] \tag{19}$$

Using Eqs. (10), (15), (16), (17) and (18) we get the control torque as follows

$$U = JG(\sigma)^{-1}[\ddot{\sigma}_d - \dot{G(\sigma)}\omega - k_1 s - k_2 sign(s) + ... \\ -\lambda\dot{\sigma}_e] + \omega^{\times} J\omega - D \tag{20}$$

To reduce the chattering in control input signal, $tanh(.)$ function is used during simulation in the place of $sign(.)$. After putting Eq. (20) in Eq. (10) the closed loop attitude dynamics is given as follows

$$\dot{\omega} = G(\sigma)^{-1}[-k_1 s - k_s sign(s) - \lambda\dot{\sigma}_e + \ddot{\sigma}_d - \dot{G}(\sigma)\omega] \tag{21}$$

5. STABILITY ANALYSIS

For position control we are using PID control law, which is a stable control law. For attitude control exponential reaching law based sliding mode control is used. We take the following Lyapunov function for proving the stability of the designed control law

$$V = \frac{1}{2}s^T s \tag{22}$$

Taking the time derivative of Eq. 22, we get

$$\dot{V} = s^T\dot{s} \tag{23}$$

Using $\dot{s}$ from Eq. (16), we get the following

$$\dot{V} = s^T(-k_1 s - k_2 sign(s)) = -k_1 s^T s - k_2|s| \leq 0 \tag{24}$$

Since the Laypunov function is negative semi-definite the the control law given in Eq. (20) is stable.

6. RESULTS AND SIMULATIONS

In this section, numerical simulations are presented for attitude and position control. Firstly, simulations are presented for attitude stabilization. Then, the simulations for space robot approaching towards a fixed position in space with respect to inertial frame are presented. Initial conditions that are used for both the simulations are provided in Table (1) and other parameters for simulation are provided in Table (2).

Parameter	Initial condition
MRP (σ_0)	$\frac{\pi}{180^0}\begin{bmatrix}15 & 6 & 10\end{bmatrix}$
Angular velocity (ω_0)	$\begin{bmatrix}0.1 & 0.1 & -0.4\end{bmatrix} rad/sec$
Position (X_0)	$\begin{bmatrix}500 & 0 & 0\end{bmatrix} m$
Velocity (V_0)	$\begin{bmatrix}1 & 1 & 0\end{bmatrix} m/sec$
Angular velocity of wheels $\begin{bmatrix}\Omega_1 & \Omega_2\end{bmatrix}$	$\begin{bmatrix}10 & 10\end{bmatrix} rad/sec$
Gimbal initial angle (γ_0)	$1 rad$

Table 1. Initial conditions for simulation

Parameter	Values
Space robot inertia	$\begin{bmatrix}1.009 & 0.25 & 0.916\end{bmatrix}\ kg.m^2$
VSCMG inertia $\begin{bmatrix}I_{1g} & I_{1s}\end{bmatrix}$	$\begin{bmatrix}0.002 & 0.03\end{bmatrix}\ kg.m^2$
Reaction wheel inertia(I_{2s})	$0.03\ kg.m^2$
k_1	2.2
k_2	0.7
λ	2.5
c_1	0.01
c_2	0.05
c_3	0.0005
Normalized inertia of asteroid	$\begin{bmatrix}61 & 43 & 514\end{bmatrix}\ m^{-2}$
Mass of asteroid	$6.1\times10^{10}\ kg$
Mass of space robot	$10\ kg$
Rotation rate asteroid (ω_T)	$0\ rad/sec$
Reference position (X_d)	$\begin{bmatrix}160 & -200 & 150\end{bmatrix}\ m$

Table 2. Constant parameter taken for simulation

6.1 Attitude Stabilization

For attitude stabilization desired MRP's σ_d are taken as $[0\ 0\ 0]^T$ and desired angular velocity ω_d as $[0\ 0\ 0]^T$. Figure. (4) shows the results of the simulations for attitude stabilization. It can be observed from Figure. 4(a) that MRP vector σ approaches to its desired values within 5 second. Angular velocity ω also reaches to its desired values within 5 sec as shown in Fig. 4(b). From Figure. 4(c) it can be observed that required torque reduces with time, as space robot reaches its desired attitude.Attitude stabilization results indicate a fast response of the inner loop. A fast response from the inner loop is desired as inner loop has to reach the commanded attitude before the next attitude set point from the outer position loop is received.

6.2 Simulations for Position Set Point

Desired position is taken as $X_d = [160\ -200\ 150]^T$m with respect to inertial frame. Initially space robot is at $X_0 = [500\ 0\ 0]^T$m in the asteroid frame. Then it starts moving towards the desired point. Firstly, required thrust vector and desired MRP's are calculated in outer loop using PID algorithm and , and desired thrust is fired. Then, in the inner loop required MRP's are achieved using VSCMG and RW. Since both commands are being executed simultaneously and it is required that desired MRP command is achieved before thrust is fired in that direction, that is why time scale separation principal is used. Simulation results for achieving desired position are shown in Fig. (5). From Fig. 5(a) it can be observed that position approaches to its desired value within 700 sec. From Fig. 5(b) it can be observed that velocity approaches to zero as space robot reaches to desired position, that implies that it stops there and start hovering. It can be seen in Fig. 5(c) that thrust reduces with time as space robot approaches to its desired position. And after that while hovering, it becomes constant.

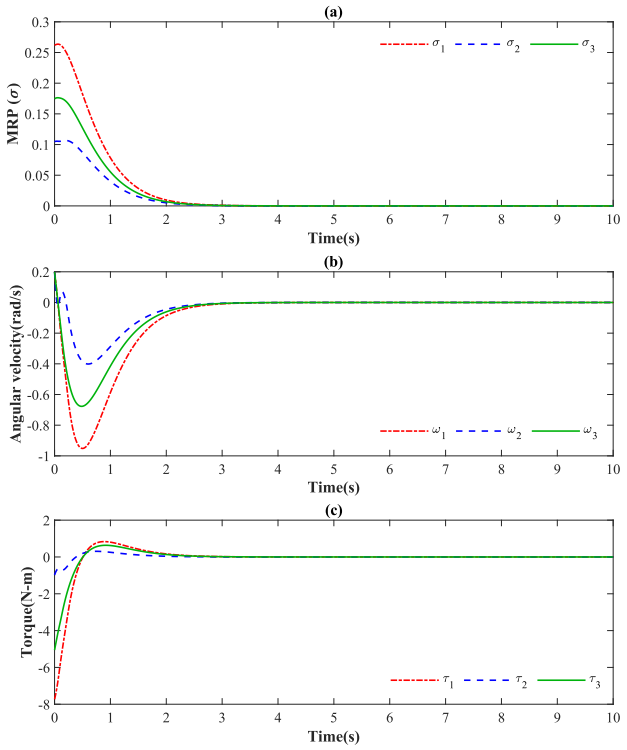

Fig. 4. Attitude stabilization

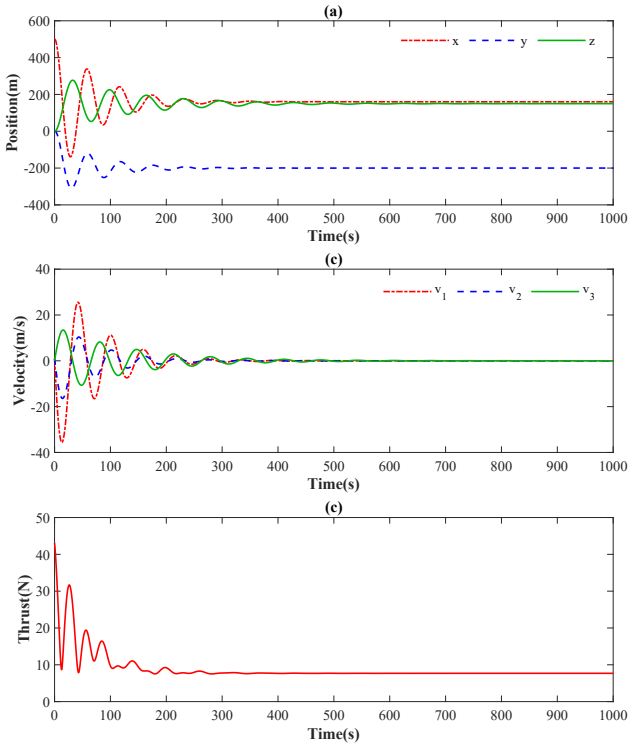

Fig. 5. Position set point approach

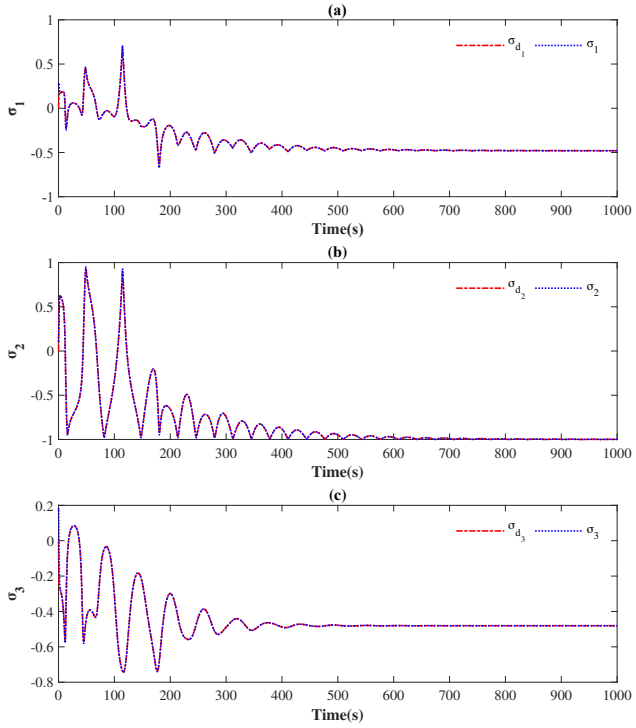

Fig. 6. MRP's for attitude tracking

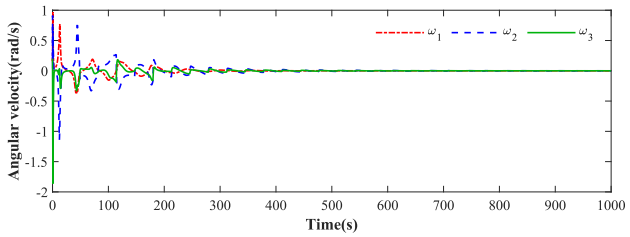

Fig. 7. Angular velocity for attitude tracking

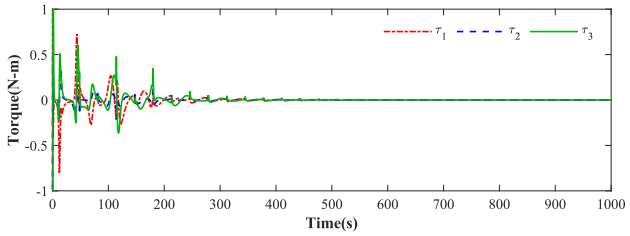

Fig. 8. Torque for attitude tracking [(τ_1) is gimbal torque, (τ_2) is gimbaled RW torque and (τ_3) is RW torque]

Results for the attitude tracking while position set point is being achived are shown in Figs. (6), (7) and. (8). Desired MRP σ_d and their corresponding response MRP σ are shown in Fig. (6). Figure (7) represents angular velocity generated for achieving the required MRP. Required torque for achieving their corresponding angular velocities are presented in Fig. (8). It can be observed that torque applied to achieve the required position is not greater than 1 N-m.

7. CONCLUSION

This paper presented an actuator configuration for asteroid exploration using one thruster, one VSCMG and one RW. As it is an under-actuated problem, control law for the system has been designed using the coupled dynamics of position and attitude control in two loops. The attitude was defined using MRP, and the system dynamics is derived using conservation of angular momentum and Newton's second law. PID control algorithm is used for postion control and attitude control law has been derived using sliding mode. To prove the stability of the system, Lyapunov stability criteria is used. Because of non-spherical body, asteroid's gravity potential is also defined to account for non-uniform gravitational acceleration. Since the position trajectory is generated by the thrust commanded by PID algorithm, it may happen that the space robot may crash on the asteroid while reaching towards it. However, this problem can be solved by developing a predefined collision free path for the system.

Future work on this problem can include optimal path planning for the space robot while scouting around the asteroid along with study of thrust misalignment of thruster and robustness of the control system.

REFERENCES

Biggs, J.D. and Livornese, G. (2020). Control of a thrust-vectoring cubesat using a single variable-speed control moment gyroscope. *Journal of Guidance, Control, and Dynamics*, 43(10), 1865–1880.

Brieß, K., Bärwald, W., Gill, E., Kayal, H., Montenbruck, O., Montenegro, S., Halle, W., Skrbek, W., Studemund, H., Terzibaschian, T., et al. (2005). Technology demonstration by the bird-mission. *Acta Astronautica*, 56(1-2), 57–63.

Cornick, D. (1979). Singularity avoidance control laws for single gimbal control moment gyros. In *Guidance and Control Conference*, 1698.

Hu, W.D. and Scheeres, D.J. (2008). Periodic orbits in rotating second degree and order gravity fields. *Chinese Journal of Astronomy and Astrophysics*, 8(1), 108.

Ismail, Z. and Varatharajoo, R. (2010). A study of reaction wheel configurations for a 3-axis satellite attitude control. *Advances in Space Research*, 45(6), 750–759.

Lungu, M. and Lungu, R. (2019). Adaptive neural network-based satellite attitude control by using the dynamic inversion technique and a vscmg pyramidal cluster. *Complexity*, 2019.

Margulies, G. (1978). Geometric theory of single-gimbal control moment gyro system. *J. Astronaut. Sci.*, 26, 159–191.

Prabhakaran, B., Kothari, M., et al. (2015). Nonlinear control design for quadrotors. In *2015 IEEE workshop on computational intelligence: Theories, applications and future directions (WCI)*, 1–6. IEEE.

Tayebi, J., Nikkhah, A.A., and Roshanian, J. (2017). Lqr/lqg attitude stabilization of an agile microsatellite with cmg. *Aircraft Engineering and Aerospace Technology*, 89(2), 290–296.

Yoon, H. and Tsiotras, P. (2006). Spacecraft line-of-sight control using a single variable-speed control moment gyro. *Journal of guidance, control, and dynamics*, 29(6), 1295–1308.